Examining aberrations due to depth of field in holographic pupil replication waveguide systems

CRAIG T. DRAPER ⓘ AND PIERRE-ALEXANDRE BLANCHE* ⓘ

College of Optical Sciences, The University of Arizona, 1630 E University Blvd, Tucson, Arizona 85721, USA
*Corresponding author: pablanche@optics.arizona.edu

Pupil expansion using waveguide propagation and pupil replication has been a popular method of developing head-up displays and near-to-eye displays. This paper examines one of the limits of pupil replication, which involves projecting images at a finite distance through a single waveguide by holographic optical elements and seeing the image doubling artifact. A Zemax model and a demonstrator were developed to determine the cause of image doubling. A relationship between the designed outcoupled image distance of a waveguide, pupil size, optical path length, and angle of image doubling is established. In waveguide pupil replication, the internally propagating light should be close to collimated to mitigate image doubling. We also provide a solution to project the image at different distances, which is an important factor for some applications, such as automotive head-up display and the seamless integration of augmented reality information with the natural environment.　© 2021 Optical Society of America

1. INTRODUCTION

Head-up displays (HUDs) and near-to-eye displays (NEDs) have become a popular area of research for mixed reality (MR) and augmented reality (AR) systems. This category of displays allows for the display of virtual information on top of the natural world [1]. Benefits can include improved situational awareness or more diverse applications, which can include social media, learning and teaching methods, and gaming [2]. They offer the ability to improve productivity by displaying relevant information on the task at hand and offer an improved bridge for human-computer interaction.

Research has been conducted to reduce the form factor of these systems where one such solution is waveguide pupil replication. Eyebox expansion by pupil replication has become an important advancement, which can also reduce the footprint of HUD and NED systems while increasing the field of view (FOV). This is particularly advantageous in NED systems where a small form factor is crucial and generally results in a small exit pupil in traditional systems [3,4].

The eyebox is defined as the three-dimensional volume over which a user can move their eyes and see the entire projected image. FOV is defined as the angular size a projected image encompasses of a user's visual system. The footprint of the system can include the waveguide coupling optics and the projector system. The exit pupil of a typical NED should be at least 15 mm in diameter to allow for the waveguide to shift while in use and allow for the user to be undisturbed by the movement as the image is still present as well as to compensate for the differences

in interpupillary distance among the human population [5]. Pupil replication can expand the small exit pupil produced by a light engine to fill the required exit pupil size. The concept of pupil duplication using a waveguide extracting recirculated light multiple times while increasing the pupil can be seen in Fig. 1. This can be applied to both the vertical and horizontal directions for a two-dimensional (2D) pupil expansion. In order for the extracted light to have a uniform brightness, the extraction efficiency should vary along the number of extractions [2]. To avoid aberration in the final image, stringent tolerances are imposed on surface defects on the waveguide since these surface errors are being compiled by the multiple interactions through total internal reflection (TIR) [6].

Among the different types of combiner elements for AR and MR applications, one can find a beam splitter, dichroic mirror, or hologram to mix the virtual and real environment. Typically, the beam splitter and dichroic mirror act as a simple reflector that puts the last optical element further from the viewer, which limits the FOV. The use of freeform optics as well as holographic optical elements allows the combiner to act as the last lens of the system, which, with every other aspect being kept equal, permits a larger FOV. However, in all these systems, the FOV and eyebox product are proportional to the finite space-bandwidth product, which implies that as when one increases the other decreases [7]. When using a waveguide to propagate the image, the light recycling inside the waveguide and the pupil replication allows us to decouple the FOV and eyebox since now the eyebox can be as large as a windshield.
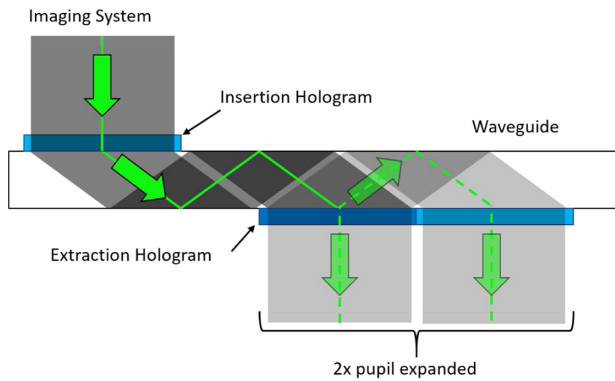
Fig. 1. Concept of 1D pupil replication where light is recirculated within the waveguide to be extracted more than once to increase the area the image can be seen.

In- and outcoupling of the light in the waveguide can be done with prisms and mirrors, but using holograms guarantees for a lighter system with a smaller form factor while being angular and wavelength selective to produce the desired wavefront [8,9]. Volume holograms can potentially have near 100% diffraction efficiency in its +1 order, reducing stray light and increasing optical efficiency [10].

A holographic waveguide system consists of an insertion hologram and an extraction hologram. The insertion hologram couples image bearing light into a planar waveguide. This light propagates through the waveguide until it interacts with the extraction hologram. The diffraction efficiency of the extraction hologram should vary along the propagation path of the light, so the same amount of light is directed toward the viewer regardless of its position in the entire extraction region. The varying diffraction efficiency preserves the image brightness across the eyebox.

For 2D pupil expansion, a redirection hologram is located between the injection and the extraction hologram. The purpose of the redirection hologram is to expand the pupil in one dimension (1D) while keeping the light inside the waveguide by redirection at 90 deg. In this case, the light that was initially traveling across the width of the waveguide is now traveling along its length, and the extraction hologram expands the pupil in the other dimension.

For a true immersion experience, the psychological and physiological visual cues must be satisfied [11]. A display should produce the physiological cues such as accommodation, vergence, motion parallax, and occlusion. This involves presenting a virtual projected image into the user's FOV to simulate an object at a certain distance from the user's perspective. If these are not satisfied, it can lead to the accommodation-vergence conflict resulting in the user being disoriented while using the display [12,13]. A method would be to display holograms to the users that satisfy all visual cues [12,14]. Other methods could be to use a mechanically shifting object plane or a pupil relayed deformable mirror to temporally multiplex image planes [15]. However, when the focal distance of the image, or the hologram, that is injected into the waveguide changes, artifacts such as image replication appear. In this paper, we examine this artifact according to the image distance using both a Zemax ray tracing model and a lab demonstrator. We propose a solution where

the image can be projected at discrete locations, allowing us to restore both vergence and accommodation cues.

2. OPTICAL SYSTEM

The optical system we are investigating is schematically represented in Fig. 1. Waveguide pupil replication is achieved using holograms laminated to a flat glass waveguide. An edge lit hologram diffracts light at an angle such that it satisfies the TIR condition. The insertion hologram receives incident image bearing light and couples the image by redirecting it to propagate internally in the waveguide. The mean angle of propagation takes the halfway point between the critical angle for TIR and when the angle is so extreme that it misses the extraction hologram. The extraction hologram outcouples light from the waveguide and directs it toward the user. The extraction hologram has segmented diffraction efficiency to extract a percentage of the light as the light propagates through the waveguide. This allows for a uniform brightness of the image as the user moves across the expanded pupil.

A waveguide has its insertion and extraction holograms designed to couple the image at a certain prescribed image distance. The injection hologram collimates the rays entering the waveguide such that the image does not suffer any (de)magnification when propagating inside the waveguide. If not so, each extraction generates an image of a different size that produces an artifact. The extraction hologram, in addition to extracting the light from the waveguide, defines the image distance of the waveguide by the focal length of the hologram. In the case of a simple grating, the image is located at infinity. To locate the image at a different distance, the extraction hologram should be given some negative optical power.

As the image distance deviates from the prescribed distance, image doubling is observed across the expanded eyebox. The angles between the doubled images were measured at the deviated distances in a Zemax ray tracing simulation and a demonstrator of a holographic waveguide display with pupil replication.

3. COMPUTER SIMULATION

The optical ray tracing program Zemax was used to model the holographic waveguide display in non-sequential mode. A 19 mm thick N-BK7 waveguide was modeled with three hologram segments: a square 50 mm × 50 mm insertion hologram and two extraction holograms. The extraction hologram consisted of two segments identical to the insertion hologram dimensions making a total size of 100 mm × 50 mm for a 2× pupil expansion. The insertion and extraction holograms were designed to propagate collimated incident light throughout the system and were modeled with Zemax's hologram lens feature. A zero diopter waveguide and a two diopter waveguide were developed with the optical parameters for the holograms listed in Table 1, which extract the image to project it at infinity and 500 mm from the extraction hologram, respectively. The recording geometry is given for the reference and object beams along with the recording wavelength, index of refraction, and diffraction efficiency of the holograms.
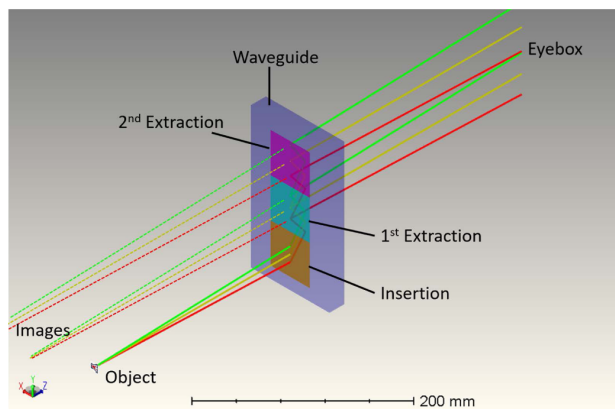
Fig. 2. Zemax layout of the pupil replicating waveguide designed for imaging at infinity. Dark blue is the waveguide, dark yellow is the insertion hologram, cyan is the first extraction hologram segment, and magenta is the second extraction hologram segment. The rays are color coded green for the upper portion of the insertion hologram pupil, yellow for the center, and red for the bottom. The rays from a single point enter the insertion hologram and produce virtual points that change in the projected distance.

Point source objects were input into the system at different distances and an imaging system was set up after the extraction hologram to find the virtual image distance as well as the angle of image doubling. The imaging system consisted of a 100 mm paraxial lens and a translatable detector plane to find the best focus at which the distance between the doubled images could be measured. The distance between the doubled images and the image distance from the paraxial lens to the detector were used to calculate the angle between the doubled images.

A waveguide designed to incouple and outcouple collimated light designed in Zemax is shown in Fig. 2. A point source object is located 250 mm in front of the insertion hologram. The extraction holograms outcouple the light, which produce a virtual object located 250 mm plus the internal propagation path length through the waveguide. Rays have been back traced to show the virtual image that each extraction hologram segment creates. Figure 3 shows the two virtual images created for an on-axis point source 250 mm from the insertion hologram. The rays differ for each image from the pupil expansion, which can both be viewed as a doubled image if the imaging system is within the indicated region of the doubled image or receives light from both extractions. The doubled image differs by an angle and projected image distance.

The projected images are shown in Fig. 4 with the object distances both matching and straying from the designed waveguide parameter. A paraxial lens collimates the $10 \text{ mm} \times 10 \text{ mm}$ object to project it at infinity. A second paraxial lens is used to induce 0.323 D of optical power to project the object at a different distance. With the image at infinity, there is no image doubling while the image at 3.4 m causes an image doubling of 0.86° seen as the horizontal direction.

The image doubling occurs immediately after the extraction of the image, and it is most visible at the location where the image is extracted by a different segment, or when a different portion of the image is extracted by the same location of the hologram. Every ray that enters the insertion hologram has its angle preserved as it propagates through the waveguide, and the
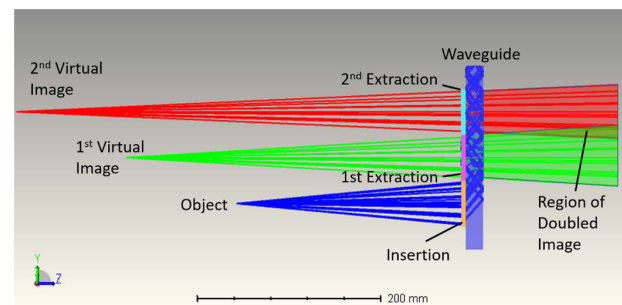
Fig. 3. Zemax layout of the pupil replicating waveguide designed for imaging at infinity. The object is at 250 mm producing two virtual images from pupil replication. The virtual images form a region of overlap where an imaging system can view both images simultaneously resulting in angularly separated image doubling.
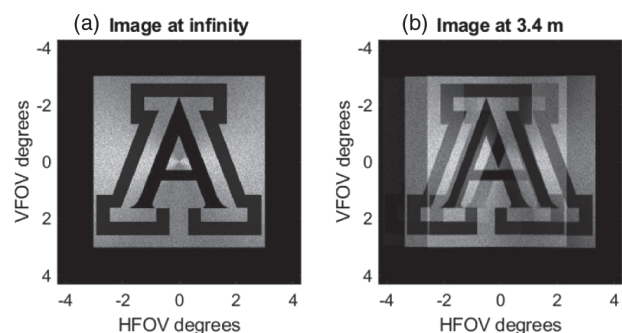
Fig. 4. The detector in a Zemax ray trace is shown here. (a) The projected image matches the designed waveguide parameter and is free from artifacts. (b) There is a mismatch between the projected image distance and the waveguide parameter causing 0.86° of difference between the doubled image.

replicated rays are extracted parallel to each other. An undisrupted image can be seen if the entire FOV of the image is only within a single extraction hologram segment. As the detector is swept across the eyebox, image doubling will be seen until the next single extraction hologram segment projects the entire FOV.

The Zemax model was altered to have a designed input and output, which allows for a virtual image to be displayed at a distance closer than infinity. In Fig. 5, a layout is shown of a system, which is designed for an object and image at 500 mm distance. A waveguide designed for a certain distance implies that the internal propagating beam within the waveguide is near collimated, but the extraction hologram acts as a negative lens. This results in no image doubling between replicated pupils as both replication segments produce an image at the same location seen in Fig. 6(a). However, when the image is projected at another distance than the prescribed 500 mm, image doubling is present as seen in Fig. 6(b). This difference in projected image depth from 500 mm to 600 mm caused 1.0° of image doubling. The object size was 40 mm x 40 mm for Figs. 6(a) and 6(b), and to preserve the virtual image size, a paraxial lens was used before the insertion hologram to add 0.33 D of optical power to project the object at a different distance.

Table 1.   Hologram Parameters for the Waveguide Display Systems Modeled in Zemax's Non-sequential Mode

	Hologram Parameters					
Waveguide	0 Diopter			2 Diopter		
Hologram	Insert	First Ext	Second Ext	Insert	First Ext	Second Ext
Type	Trans	Reflect	Reflect	Trans	Reflect	Reflect
X_{ref} (mm)	0	0	0	0	0	0
Y_{ref} (mm)	−1.35E8	0	0	−1.35E8	0	0
Z_{ref} (mm)	1E8	1E8	1E8	1E8	740.75	740.75
X_{obj} (mm)	0	0	0	0	0	0
Y_{obj} (mm)	0	−1.35E8	−1.35E8	0	−1.35E8	−1.35E8
Z_{obj} (mm)	1E8	−1E8	−1E8	759.75	−1E8	−1E8
λ_{rec}/n (μm)	0.35	0.35	0.35	0.35	0.35	0.35
n	1.5	1.5	1.5	1.5	1.5	1.5
Efficiency %	100	50	100	100	50	100
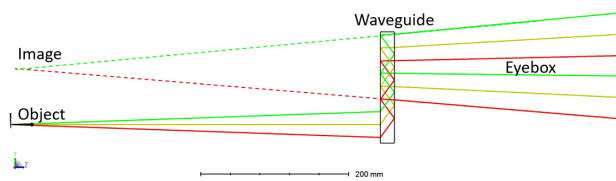
Fig. 5. Layout of a Zemax model of a waveguide designed to incouple light at an object distance of 500 mm and project it virtually at 500 mm. Back tracing the rays shows that the eyebox creates a single virtual image point.
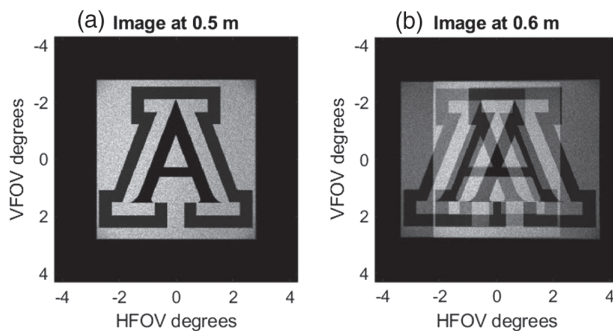
Fig. 6. (a) The projected image is matching the designed waveguide parameter and has no artifacts. (b) The projected image does not match the waveguide parameter and has 1.0° of difference between the doubled image.

4. PROOF OF CONCEPT DEMONSTRATOR

Three holograms were recorded on a 19 mm thick glass waveguide using a 16 μm Covestro Bayfol photopolymer. The insertion hologram is a square with dimensions of 50 mm × 50 mm. The extraction hologram total size is 50 mm × 100 mm. There is no spacing between the hologram segments. A grating period of 0.298 um is recorded into 16 μm thick photopolymer material to achieve an edge lit hologram using a frequency doubled YAG coherent laser at 532 nm.

The insertion hologram was recorded using a coupling prism for the collimated object beam and a collimated normally incident beam as the reference beam. The angle of the object beam was set at 53.5°, which is the median angle between the TIR angle and the angle at which internally propagating light would

Fig. 7. Demonstrator showing three segments of coupling holograms named the insertion and first and second extraction holograms. Each hologram is laminated to an N-BK7 waveguide.

miss the extraction holograms. To achieve this recording angle, a coupling prism was index matched to the waveguide during the recording process of the insertion hologram.

The extraction hologram consisted of two segments, which expanded the pupil in 1D by 2×. The extraction holograms were recorded using a collimated single large beam, which served as the object beam. The reference beam was formed from the resulting collimated diffracted light from the insertion hologram. The layout of the holograms on the waveguide can be seen in Fig. 7.

5. RESULTS

The image doubling was captured in Zemax by varying the object distance and recording the pixel shift between the two objects created. The image doubling was captured in the demonstrator by moving the object plane of the projector to produce virtually projected images at different distances. The angular differences in the images were measured against the virtually projected image distance using the imaging equation, which relates object distance, image distance, and focal length. The object used was a 1951 Air Force Resolution Target (ARFT). Figure 8 shows similar amounts of image doubling
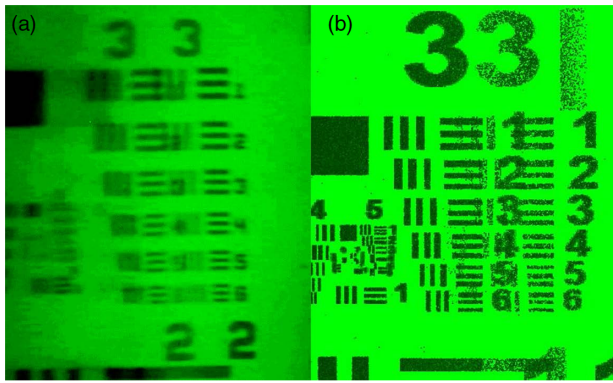
Fig. 8. Left image (a) is contrast enhanced and shows image doubling of an Air Force Resolution Target in the demonstrator captured with a digital single lens reflex camera while the right image (b) shows image doubling of a simulated Air Force Resolution Target in the Zemax ray tracing model.

Fig. 9. Plot showing the angle between the doubled images due to adjusting the object distance to produce a virtually projected image at assorted distances.

resulting from the demonstrator and the simulation of group 3 of the AFRT.

An angle was calculated from the difference in the doubled image to find a relationship between the object distance and the image doubling denoted α. This led to a theoretical equation describing the relationship seen in Eq. (1). Equation (2) describes the effective size of the pupil from pupil replication,

$$\alpha = 2\arctan\left(\frac{\text{pupil}}{-2z_i}\right), \tag{1}$$

$$\text{pupil} = L(N-1), \tag{2}$$

where z_i is the virtually projected image distance in millimeters, which is negatively signed in accordance to the sign convention of a Cartesian coordinate system. L is the insertion hologram size in millimeters in 1D multiplied by the number of extraction hologram segments N where the term N is rounded up to the nearest integer.

The user's eye accommodation is the variable ϕ, which is in units of diopters to see the object at the projected distance as shown in Eq. (3). The eye accommodation is defined as the inverse of the negative image distance with a conversion factor from inverse millimeter to diopter. A linear correlation was realized when using the user's eye accommodation as the independent variable instead of the virtual image distance,

$$\alpha = 2\arctan\left(\frac{\text{pupil}}{2}\frac{\phi}{1000}\right). \tag{3}$$

The angle found in the demonstrator and the Zemax simulation is compared to the theoretical equation in Fig. 9. The parameters are that the pupil is 50 mm and the image distance range was from -3.4 m to $-\infty$. It is seen that as the image distance approaches infinity, the image doubling approaches zero. The point where the image is at infinity and the image doubling is 0 was intentionally left out to be able to see the trend at lesser image distances.

It is seen that upon analysis of a waveguide, which was designed to produce a virtual image other than at infinity, the optical path length from the extraction pupil becomes a factor in
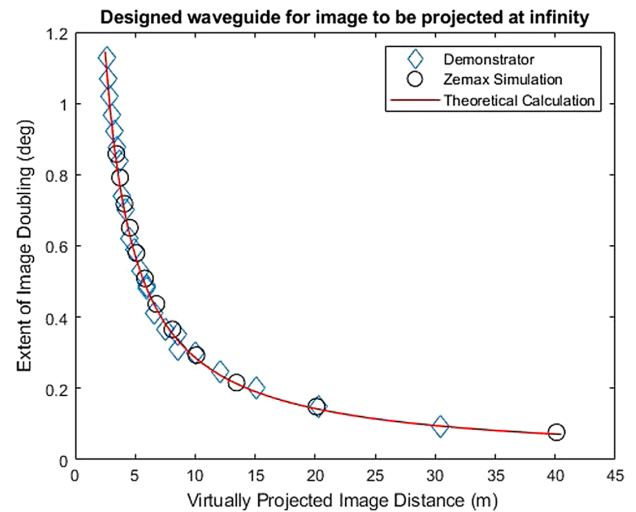
the image doubling as well as the designed image distance of the waveguide display. This relationship is shown in Eq. (4),

$$\alpha = 2\arctan\left[\left(\frac{1}{z_w}+\frac{1}{z_i}\right)\frac{\text{pupil}}{2}\left(1-\frac{t}{z_w}\right)\right]. \tag{4}$$

The variable z_w is the designed projected distance of the waveguide and extraction holograms in millimeters. It is negative as it is a virtually projected distance. The variable t is the optical path length from the extraction hologram to the user's pupil in millimeters.

Equation (4) can be rearranged to find the depth range that can propagate through a waveguide by setting the angle of image doubling to 1 arc min. At this angle, any image doubling would be unnoticeable to the user as this is the limit of the visual acuity of a standard human observer [16].

A waveguide display used to outcouple a virtual image at 0.5 m was simulated in Zemax. The image doubling as a function of image distance was observed by varying the object distance from the waveguide insertion hologram and viewing the produced image after the extraction holograms. This was plotted against the relationship shown in Eq. (5) in Fig. 10. To demonstrate this effect in the lab, we simply placed a 0.5 m negative lens after the extraction hologram. The parameters considered were a pupil of 50 mm, an optical path length of 28.9 mm, z_w of -500 mm, and a z_i range from -433 mm to $-\infty$ mm. The data point at infinity is not shown in the plot.

6. DISCUSSION

The root of the image doubling artifact comes from the fact that the different rays originating from a single point of the image are not propagating collimated inside the waveguide. During the extraction, the rays extracted first are forming a different image from the image formed from the replicated rays extracted later on during the pupil expansion process. The cause of the image doubling when the image is projected at a distance different from which the waveguide is intended for can be seen in
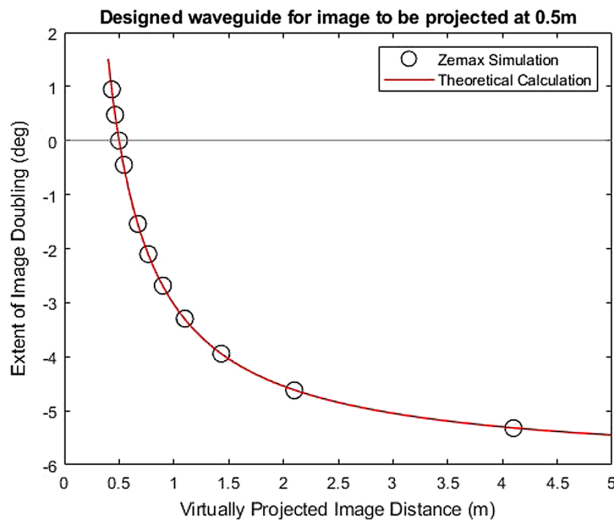
Fig. 10.   Plot showing the angle between the doubled images due to adjusting the object distance to produce a virtually projected image at assorted distances for a waveguide display designed to project an image at 0.5 m.

Fig. 11.   Log scaled plot showing the image depth range that can be transmitted by a waveguide display with pupil replication according to the designed image distance of the waveguide display. The difference between effective pupil sizes is shown. These are related to the depth perception of the standard observer based on binocular disparity.

Fig. 3. Each replicated pupil creates its own image of the original object. If the object is a centered point source, each replicated pupil will create a centered point source relative to each replicated pupil. When viewing the extracted image, a pair of point sources can be seen separated by an angle based on the position of these point sources relative to each other.

Each segment of the extraction hologram produces its own virtual object. If the detection system is placed directly behind one of the segments of the extraction holograms, a single point is seen from the object. If the detection system is placed between the segments of the extraction holograms, light rays enter the detection system from both segments and are viewed as two offset points in the direction of pupil replication. The angular difference between these points is causing image doubling.

Equation (4) can be rearranged to find the range of depth that can be put into a waveguide by solving for the variable z_i and setting the angle between the doubled images to 1 arc min to be unnoticeable to the user based on visual acuity. The difference between the image distances for positive and negative values of 1 arc min can be used to find the depth range, and this can be approximated by Eq. (5),

$$\Delta z \approx 2 \left\{ \left[\left(\frac{1}{z_w} - \frac{2}{\text{pupil}} \right) * \frac{\tan(\frac{\alpha}{2})}{1 - \frac{t}{z_w}} \right]^{-1} - z_w \right\}. \quad \textbf{(5)}$$

The depth range relationship can be used to find the depth of field in which a waveguide display can transmit without inducing noticeable image doubling across the expanded eyebox by pupil replication. Figure 11 shows the depth range in which a waveguide can transmit according to its extraction hologram's focal length. As the extraction hologram's focal length decreases, the depth range decreases. As the pupil size is decreased, a larger depth range can be transmitted before noticeable image doubling occurs. A shorter optical path length from the extraction holograms to the user's entrance pupil will also increase the depth range.
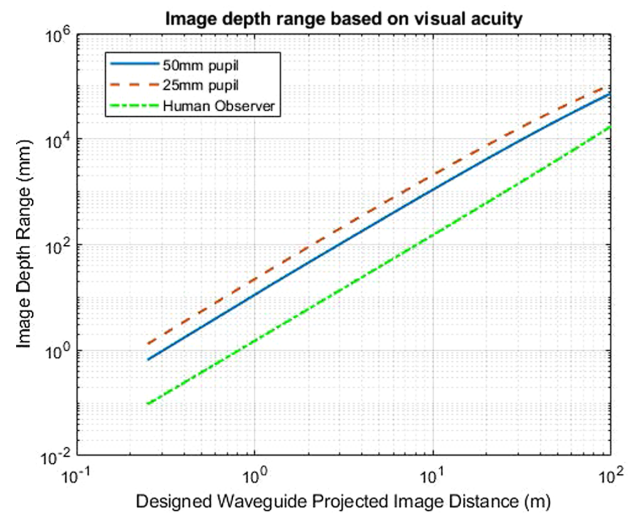
As can be seen from Fig. 11, the depth range is extremely limited: 1/100 of the projected distance for a 50 mm pupil and 1/50 for a 25 mm pupil. These ranges can be compared to the standard observer's depth perception based on binocular disparity. According to [17], the angular acuity of a person is 20 arc sec for normal vision. The approximation for angular disparity based on geometry given by [18] can be rearranged to solve for the depth between two objects shown in Eq. (6). The relation between viewing distance and depth range for the standard observer is plotted against the depth range of an artifact minimized pupil replicating waveguide system. The variables are defined as follows: Δd is the depth range, D is the image distance, I is the interpupillary distance, and δ is the angular acuity. It can be seen that the standard observer may be able to view depth information from a single pupil replicating waveguide,

$$\Delta d \approx \frac{D^2 \delta}{I - D\delta}. \quad \textbf{(6)}$$

A possible way to overcome the limitation of depth range within a single waveguide display is to use multiple waveguides in a multi-focal configuration. A Zemax simulation was constructed with two waveguides, one designed for projecting the image at −2.1 m, and the other projecting the image at infinity. For this model, the insertion holograms between waveguides were spatially separated to avoid cross talk while the extraction holograms were overlaid for the images to appear to be in the same FOV. Since the insertion holograms are spatially separated, multiple light engines are required to produce each depth plane. Alternatively, a single light engine can be used with different sections of the image injected by the different input holograms. The output images are shown in Fig. 12 over a 2× expanded pupil. Notice there is no image doubling with two distinct projected image distances. Using this waveguide multiplexing technique, multiple images can be projected at different distances respecting both the accommodation and the vergence optical cues for the viewer. Considering the waveguide used in
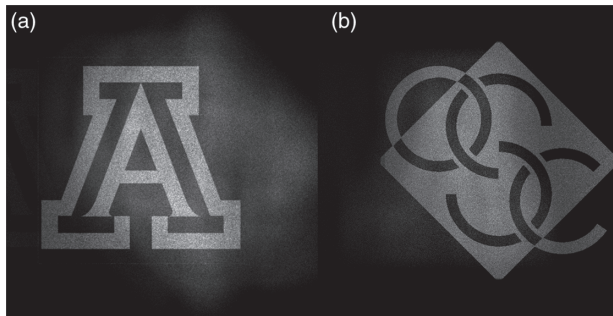
Fig. 12. Zemax simulated images with two depth sceneries overlaid on another. Left, University of Arizona symbol imaged at 2.1 m; right, College of Optical Sciences logo imaged at infinity.

HUD and AR glasses can be as thin as a fraction of a millimeter, this technique does not make the combiner too bulky or heavy. For a sufficiently large depth of field from 0.33 m to infinity, six waveguides can be used [19].

For the sake of this example, we have chosen a set of parameters for the waveguide where the image doubling phenomenon is quite distinct and can be clearly visualized. However, it has to be kept in mind that for other parameters such as injection angle and waveguide thickness, the image doubling phenomena can be more acute and visually complex.

7. CONCLUSION

Image doubling is observed in pupil replicating holographic waveguide displays when the internal propagation within the waveguide is not collimated. The limit of image splitting is set by the user's ability to detect an angular difference, which is set by the human visual acuity. We showed that this tolerance is extremely small, and the image depth range can only be a small fraction of the projection distance (1/50). Propagation of larger depth ranges will result in image doubling across an expanded pupil.

The depth range that can propagate through a pupil replicating waveguide is limited by the designed waveguide projected image, the pupil size, the optical path length from the extraction hologram to the user's detection system, and the tolerable angular displacement between doubled images.

To have a MR experience, multiple waveguides, where each is for a different image depth, should be used if pupil replication is desired.

Disclosures. The authors declare no conflicts of interest.

REFERENCES

1. P. Milgram and F. Kishino, "A taxonomy of mixed reality visual displays," IEICE Trans. Inf. Syst. **77**, 1321–1329 (1994).
2. C. T. Draper, C. M. Bigler, M. S. Mann, K. Sarma, and P.-A. Blanche, "Holographic waveguide head-up display with 2-D pupil expansion and longitudinal image magnification," Appl. Opt. **58**, A251–A257 (2019).
3. W. Zhang, C. P. Chen, H. Ding, L. Mi, J. Chen, Y. Liu, and C. Zhu, "See-through near-eye display with built-in prescription and two-dimensional exit pupil expansion," Appl. Sci. **10**, 3901 (2020).
4. L. Gu, D. Cheng, Q. Wang, Q. Hou, and Y. Wang, "Design of a two-dimensional stray-light-free geometrical waveguide head-up display," Appl. Opt. **57**, 9246–9256 (2018).
5. J. E. Melzer, F. T. Brozoski, T. R. Letowski, T. H. Harding, and C. E. Rash, "Guidelines for HMD design," in *Helmet-Mounted Displays: Sensation, Perception, and Cognition Issues*, C. E. Rash, M. Russo, T. Letowski, and E. Schmeisser, eds. (U.S. Army Aeromedical Research Laboratory, 2009), pp. 805–848.
6. T. Levola, "Diffractive optics for virtual reality displays," J. Soc. Inf. Disp. **14**, 467–475 (2006).
7. C. Chang, K. Bang, G. Wetzstein, B. Lee, and L. Gao, "Toward the next-generation VR/AR optics: a review of holographic near-eye displays from a human-centric perspective," Optica **7**, 1563–1578 (2020).
8. I. Kasai, Y. Tanijiri, T. Endo, and H. Ueda, "A practical see-through head mounted display using a holographic optical element," Opt. Rev. **8**, 241–244 (2001).
9. S. Lee, B. Lee, J. Cho, C. Jang, J. Kim, and B. Lee, "Analysis and implementation of hologram lenses for see-through head-mounted display," IEEE Photon. Technol. Lett. **29**, 82–85 (2017).
10. R. Kostuk, *Holography: Principles and Applications*, Series in Optics and Optoelectronics (CRC Press, 2019).
11. J. Hong, Y. Kim, H.-J. Choi, J. Hahn, J.-H. Park, H. Kim, S.-W. Min, N. Chen, and B. Lee, "Three-dimensional display technologies of recent interest: principles, status, and issues [invited]," Appl. Opt. **50**, H87–H115 (2011).
12. Y. Su, X. Tang, Z. Zhou, Z. Cai, Y. Chen, J. Wu, and W. Wan, "Binocular dynamic holographic three-dimensional display for optical see-through augmented reality using two spatial light modulators," Optik **217**, 164918 (2020).
13. T. Shibata, J. Kim, D. M. Hoffman, and M. Banks, "The zone of comfort: predicting visual discomfort with stereo displays," J. Vis. **11**(8):11 (2011).
14. K. Wakunami, P.-Y. Hsieh, R. Oi, T. Senoh, H. Sasaki, Y. Ichihashi, M. Okui, Y.-P. Huang, and K. Yamamoto, "Projection-type see-through holographic three-dimensional display," Nat. Commun. **7**, 12954 (2016).
15. X. Hu and H. Hua, "High-resolution optical see-through multi-focal-plane head-mounted display using freeform optics," Opt. Express **22**, 13896–13903 (2014).
16. C. M. Fidopiastis, C. Meyer, C. A. Fuhrman, and J. P. Rolland, "Quantitative assessment of visual acuity in projective head mounted displays," Proc. SPIE **5079**, 399–406 (2003).
17. B. M. S. Deepa, A. Valarmathi, and S. Benita, "Assessment of stereo acuity levels using random dot stereo acuity chart in college students," J. Family Med. Primary Care **8**, 3850–3853 (2019).
18. S. Palmisano, B. Gillam, D. G. Govan, R. S. Allison, and J. M. Harris, "Stereoscopic perception of real depths at large distances," J. Vis. **10**(6):19 (2010).
19. S. Liu and H. Hua, "A systematic method for designing depth-fused multi-focal plane three-dimensional displays," Opt. Express **18**, 11562–11573 (2010).